ELSEVIER

Journal of Electroanalytical Chemistry 431 (1997) 51–56

JOURNAL OF ELECTROANALYTICAL CHEMISTRY

Preliminary Note

The growth of the second underpotentially deposited silver layer on Pt(100)

A.M. Bittner *

Fritz-Haber-Institut der Max-Planck-Gesellschaft, Faradayweg 4-6, D-14195 Berlin, Germany

Received 8 April 1997; revised 5 May 1997

Abstract

The electrodeposition of Ag on Pt(100)-(1 × 1) in perchlorate electrolyte was studied by means of time-resolved in situ scanning tunnelling microscopy (STM) and cyclic voltammetry. One monolayer of Ag is deposited underpotentially (upd) ca. 500 mV positive of the Ag^+/Ag equilibrium potential. Several millivolts positive of the equilibrium potential, a second well defined upd layer forms. Its growth was observed to proceed via island formation and coalescence. This process occurs in two separate stages that manifest themselves in voltammetric peaks as well as in the STM images. © 1997 Elsevier Science S.A.

Keywords: Cyclic voltammetry; Film growth; Scanning tunnelling microscopy (STM); Single crystal electrode; Surface structure; Underpotential deposition (upd)

1. Introduction

The metal-on-metal deposition from electrolytes is a most important technical process employed in the finishing industry for plating and microelectronic devices. To elucidate its foundations, research has been using single crystalline surfaces of noble metals as substrates that can easily be investigated with scanning tunnelling microscopy (STM). Especially well documented is the case of Cu deposition on Au(111) [1–9]. Here, and in many other cases, a monolayer adsorbs even when positive of the bulk deposition potential (underpotential deposition, upd). Usually, anions from the electrolytes can coadsorb; in fact, they even play a crucial role for the formation of ordered upd monolayers. For example, it is quite likely that during the deposition first a highly mobile metal adion or adatom layer forms (both with coadsorbed anions). At a certain potential (often close to the upd peak potential) a phase transition occurs and an ordered immobile film — comprising metal adatoms or adions and coadsorbed anions — covers all of the surface [10]. As for metal-free anion adsorbate layers (e.g. halogenides [11,12] or sulphate [13]), incomplete upd layers (e.g. islands) are therefore very rarely observed. A rare exception is the island formation for the Cu upd on Au(111) that is found when Na_2SO_4 rather than H_2SO_4 electrolyte is employed [9]. Islands can also be induced at very low adsorbate concentrations, as known for Cu/Au(111) in H_2SO_4 [10]. Often coadsorbed anions desorb at lower (still upd) potentials and the metal monolayer is completed to a (1 × 1) structure.

For Ag on Au(111) [5,14,15] and on Pt(111) [16,17] it is well established that the upd occurs at very positive potentials where it forms a complete layer. In contrast to Cu upd, a second Ag upd process is observed on Pt(111). It is situated only several 10 mV from the Ag bulk deposition and leads to a second Ag layer [16,17]. Similar effects are observed with an iodated Pt(111) substrate [18].

Fcc(100) substrates are less commonly employed, despite the fact that their more open square structure can lead to otherwise inaccessible square-shaped upd layers [19] and are known to induce relaxation effects in multilayers [20]. The Ag upd on Pt(100) was studied by El Omar et al. [17] with cyclic voltammetry and Auger electron spectroscopy.

For this study Ag was electrodeposited on a Pt(100) surface and the film structure was followed by in situ electrochemical STM and simultaneous cyclic voltammetry. Only images recorded at fixed potentials are presented, although they were also recorded during potential scans.

* Present address: Institut de Physique Expérimentale, Dépt. de Physique, École Polytechnique Fédérale de Lausanne, CH-1015 Lausanne-Ecublens, Switzerland. E-mail: alexander.bittner@ipe.dp.epfl.ch.

PII S0022-0728(97)00269-6

The film thickness ranged from a monolayer to 3D clusters. Since in our study, and in [17], the sample was flame annealed and quenched in water without potential control, the deposition takes place on the unreconstructed Pt(100)-(1 × 1) substrate [20]. The hexagonal reconstruction of Pt(100) has been shown to be preserved in contact with the electrolyte only when the sample, after preparation in vacuum, is kept at negative potentials; it is lifted irreversibly under any other condition [21,22].

2. Experimental

STM measurements were performed with a home-built instrument described in [12]. The relevant experimental details can be found in [11,20]. A new feature was that the Pt wire quasi-reference was immediately covered with an Ag layer since its open circuit potential (OCP) is lower than that of the Ag upd on polycrystalline Pt; thus the reference's potential almost matched the Ag bulk deposition potential of 620 mV vs. SHE. All potentials are quoted with respect to the standard hydrogen electrode (SHE). Electrolytes were prepared from 70% $HClO_4$ (Suprapur, Merck), $AgClO_4 \cdot H_2O$ (puriss., Fluka) and triply distilled water.

3. Results and discussion

3.1. Cyclic voltammetry

After flame annealing to yellow heat and cooling in air to dark red heat, the crystal was quenched in water, resulting in a Pt(100)-(1 × 1) surface [20]. The use of perchlorate electrolyte in this work and the use of stronger adsorbing sulphate by El Omar et al. in their study of Ag upd on Pt(100) [17] may result in small voltammetric differences which, however, should not prohibit a comparison. The potential region of the first upd process at ca. 1100 mV vs. SHE [17] was avoided in order to prevent a possible oxidation of the substrate that might interfere with deposition processes. Since the Pt was immersed at open circuit potential (800–900 mV vs. SHE), it was covered with roughly one monolayer (1 ML) of Ag [17] that had adsorbed spontaneously. Fig. 1a shows a cyclic voltammogram of Pt(100) in 100 mM $HClO_4$ + 1 mM $AgClO_4$ which was recorded in the STM electrochemical cell. The features at potentials negative of 620 mV are caused by Ag bulk deposition and dissolution. The rightmost peak is caused by stripping of the second Ag upd layer [17]. The position of the corresponding cathodic peak close to the bulk deposition potential (only 7 mV positive, see also [17]) suggests that — different from most other upd processes, but in common with Ag upd on Pt(111) [16,17] and Pt(110) [17] — even the second Ag layer has not attained the properties of bulk Ag. The upd is somewhat sluggish, due to the fact that slightly faster potential scans (e.g. 20 mV/s) shift the peak to more negative potentials and broaden it. The charge evaluated from the upd peak amounts to ca. 160 $\mu C \cdot cm^{-2}$ (see also [17]) while 208 $\mu C \cdot cm^{-2}$ is equivalent to 1 ML of Ag atoms (1 Ag atom per Pt surface atom). One can assume that the charge results almost solely from Ag deposition and is not due to coadsorbate (water or perchlorate) reorganisation or desorption, although it is not possible to rule out such contributions. However, if any coadsorbate is present, it should be very little since both perchlorate and water are weak adsorbates (e.g. no superlattices as for sulphate have been imaged with STM on Au(111)). Fig. 1b shows that the voltammetric behaviour depends critically on the potential scan speed: at 1 mV/s the peak can be resolved into two sub-peaks, C II and C III, which have never been reported before. Obviously, the growth of the second Ag layer occurs in two distinctly separated processes. As proven by the window opening experiment of Fig. 1b, process II, which deposits and strips ca. 0.5 ML of Ag can be evoked (C II) and reversed (A II) without triggering process III (ca. 0.25 ML). In a further cathodic scan the diffusion-limited bulk deposition peak is quickly reached and rather sharp (as also found by El Omar et al. [17]); in other words, Ag bulk deposition is a fast process. The evolution of H_2 on bulk Ag starts below ca. −200 mV vs. SHE.

3.2. Second layer growth

Owing to the simultaneous recording of STM images and voltammograms, one can easily correlate STM data with electrode potentials even though the potentials of interest are very closely spaced (some millivolts, see Fig. 1b). It is worth noting that STM images tended to be rather noisy and streaky since the tip often made more than one jump per scan line, rendering atomic resolution impossible. An explanation may be provided by the rapid diffusion of Ag adatoms under the STM tip [23]. Starting at 660 mV (Fig. 2a), STM images show the usual step geometry of Pt(100) [11,20]: monolayer height (0.20 nm) steps separate terraces which appear in different grey shades (easily seen around the rhombus-shaped terrace at the right-hand side). Some double and triple steps can be recognized by the frequent occurrence of a 90° angle (e.g. in the middle part) running in a zig-zag fashion from top to bottom. It should be clarified that all following STM observations are valid for areas with or without multiple steps and for small or large terraces. The already deposited 1 ML of Ag has formed a smooth layer and thereby followed the Pt topography. Note that the step heights of Pt (0.196 nm) and Ag (0.205 nm) are too similar to be distinguished. Some bright protrusions (height up to 0.2 nm, diameter ca. 4 nm) are also seen. Their density (ca. 0.02 nm^{-2}) is more than ten times lower than the density of the naturally occurring immobile hillocks (height ca. 0.2 nm, diameter 1–1.5 nm) that cover the freshly prepared clean Pt(100) surface and

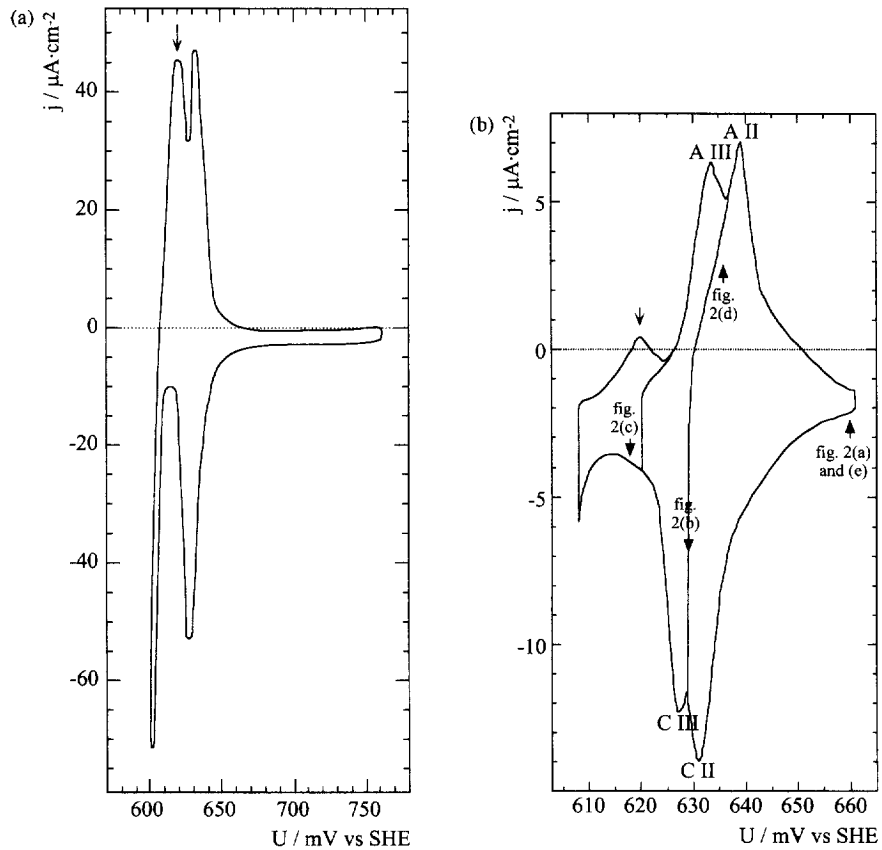

Fig. 1. Cyclic voltammograms showing the deposition and stripping of the second upd Ag layer on flame-annealed and water-quenched Pt(100) in 1 mM $AgClO_4$ + 100 mM $HClO_4$. The first upd layer forms at ca. 1100 mV (not shown) while bulk Ag is stripped at 620 mV vs. SHE (see arrows). Traces of O_2 produce a small negative offset of the current. Recorded in the STM cell. (a) Potential scan speed 5 mV/s. An anodic and cathodic second Ag layer peak appear at 632 and 627 mV vs. SHE. (b) Cathodic window opening experiment at 1 mV/s. The anodic trace shows the bulk dissolution peak (arrow) and the second layer dissolution peak which is resolved into two sub-peaks A II and A III (639 and 634 mV vs. SHE). Note that the appearance of the cathodic peak C II (631 mV vs. SHE) already suffices to produce A II. C III peaks at 627 mV vs. SHE.

should consist of Pt adatoms [20]. Since the protrusions are on average much larger than the Pt hillocks, it is likely that they are Ag islands (i.e. already second layer Ag atoms!) which are pinned to the immobile substrate hillocks. Hence, these Ag islands are due to substrate features. They also coalesced and thereby reduced their density below that of the Pt hillocks. The Ag island coverage of ca. 0.25 ML on top of the first Ag layer leaves 0.75 ML Ag to complete the second layer in the upd peaks C II and C III: indeed, this coverage was measured (see above). From this it is reasonable to assume that the second layer upd process leads again to a closed (1 × 1) layer of Ag atoms, as also observed for the Pt(111) substrate [16].

Upon setting the potential between peak C II and C III, one would expect 0.25 ML + 0.5 ML = 0.75 ML of Ag in the second layer. This means that the Ag film cannot be complete. The question arises which structure it takes on. The STM provides the following answer: First the growth of Ag islands sets in, and after several seconds an image as seen in Fig. 2b results (on a time scale of minutes some further coalescence may occur). The surface is now covered by monolayer high, partially coalesced islands similar to the structures encountered in metal-on-metal deposition in vacuum. The resolution of the images is too low to detect the phenomenon of 'frizzy steps'; that is, the high mobility of Ag step atoms [23]. Such an effect — although as yet only shown for a bulk Ag substrate with and without a Cu layer — should evoke a compact island form, as indeed is the case. Since Ag can nucleate not only at steps but also on top of existing second-layer Ag, one could still expect 3D growth. Instead, one finds a smooth deposit, as in Ag(100) homoepitaxy [24,25], which can be attributed to the rapid diffusion across a step that was recently predicted for a Ag(100) substrate [26]. It proceeds via an exchange process, is as fast as the Ag adatom diffusion on terraces and should, even for Ag bulk growth lead to compact, square-shaped islands.

Since here the substrate is a upd layer (i.e. neither bulk Pt nor bulk Ag) and an electrolyte is present, the growth mode is complex. In particular, the question why the Ag film is not completed, but forms islands, remains open. The unusual observation of upd islands could be connected with the use of perchlorate that adsorbs more weakly than, for example, sulphate. This is bolstered by the fact that the

typical sudden condensation (without islands) of a metal–anion coadsorption phase (as, e.g., known for Cu/Au(111) in sulphate electrolyte [10]) does not happen here. A tentative explanation is that Ag adatoms carry no coadsorbate and thus can attract each other in the same way as in vacuum deposition. Since almost no third layer Ag was observed, the interlayer transport is fast (i.e., Ag adatoms on a Ag terrace diffuse rapidly across a step in accordance with [25,26]); additionally the high exchange current of a Ag surface could smoothen the surface [23]. Because a part of the steps in Fig. 2a has moved, the growth should at least partially have started at the steps of the first monolayer and thereby have changed the step structure.

In summary, the growth appears to be composed of step flow (the latter process), island formation and enlargement of the already existing Ag islands. Ag could have nucleated at Ag steps and on Ag terraces. In either case can it diffuse rapidly on terraces and across steps.

3.3. Second-layer completion

When peak C III is reached (Fig. 2c), 0.25 ML Ag adsorb and the surface appears almost as in Fig. 2a, but without the protrusions — obviously it is now almost completely covered by two smooth layers of Ag. Apart from several holes, only some irregularly shaped gaps close to the substrate steps remain in the second Ag layer. Fig. 3 shows an image that was recorded under similar conditions, only on a larger scale. In the upper middle part the typical double and triple rectangularly shaped steps are found (they reflect the Pt substrate topography). Some terraces are only covered by small Ag islands while a large, coarsely structured Ag island has assembled on the terrace on the left. The topography almost resembles Fig. 2b since the gaps between steps and island boundaries are large. These gaps of Fig. 2c and Fig. 3 could be caused by a strain phenomenon [20] since a pseudomorphic Ag layer

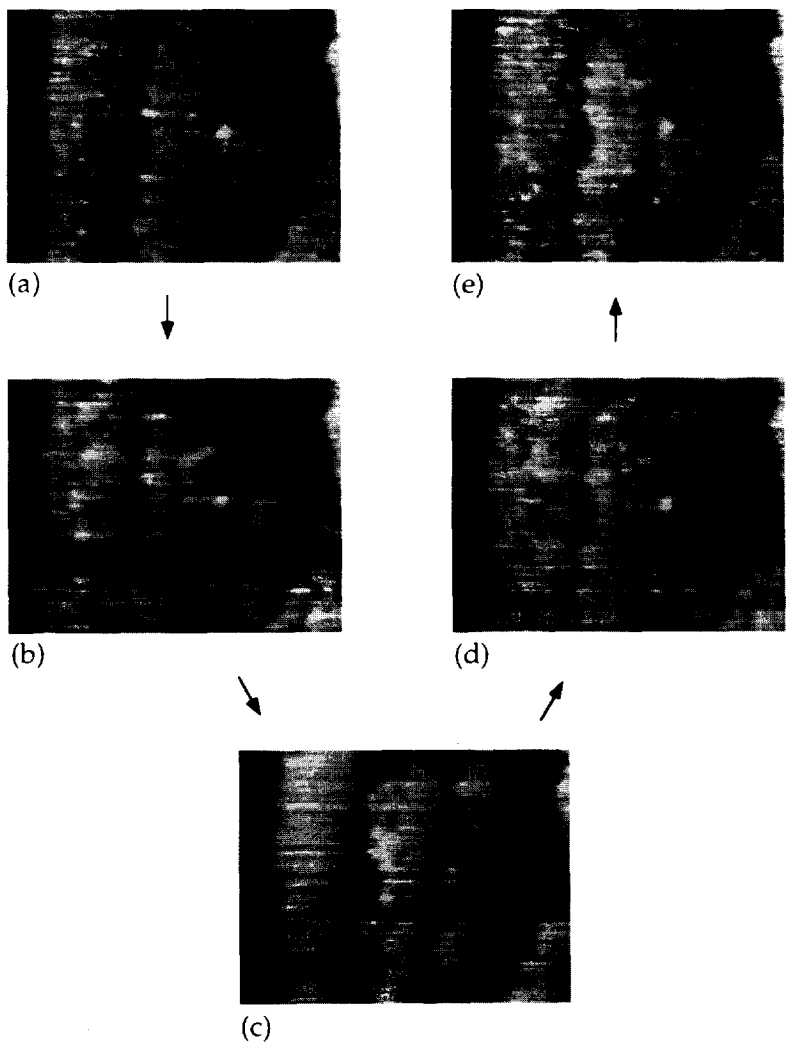

Fig. 2. Consecutively recorded STM images (each 50 s) of Pt(100) in 1 mM $AgClO_4$ + 100 mM $HClO_4$ showing the deposition of a layer of Ag. 136 nm × 104 nm, tip potential 615 mV vs. SHE, tunnelling current 10 nA. Counter-clockwise: (a) 660 mV vs. SHE, positive of peak C II; (b) 629 mV vs. SHE, negative of peak C II; (c) 618 mV vs. SHE, negative of peak C III; (d) 636 mV vs. SHE, positive of peak A III; (e) 660 mV vs. SHE, positive of peak A II.

Fig. 3. STM image of Ag islands on Pt(100) in 1 mM $AgClO_4$ + 100 mM $HClO_4$ at 620 mV vs. SHE. 153 nm × 142 nm, tip potential 609 mV vs. SHE, tunnelling current 27 nA.

is compressively strained (Ag–Ag: 0.289 nm, Pt–Pt: 0.277 nm). Atomically resolved images (yet to be obtained) should assist in elucidating this phenomenon [20].

3.4. Second-layer dissolution

As shown in Fig. 2d, the former state (Fig. 2b) can easily be reached again by sweeping back through peak A III. Due to the stochastic nature of the adsorption, the islands take on different forms and locations than in Fig. 2b. Finally, after sweeping through peak A II and desorbing the Ag, the image (Fig. 2e) becomes almost identical to Fig. 2a. This means that the second Ag layer deposition is reversible, except that it leaves again ca. 0.25 ML of second-layer Ag at almost the same positions as before, a further indication that the immobile hillocks (i.e. defects) on Pt(100) act as nucleation sites for Ag.

3.5. Bulk deposition

The deposition of bulk material (the tip was retracted to avoid shielding effects [20]) results in extended 3D islands. Unlike Cu/Pt(100) (see fig. 9 of [20]), step lines can only be detected in some cases, although the Ag bulk structures are not very rough, which is unusual for 3D growth. Since bulk Ag can also form rather smooth deposits on Pt(111) [16] and Au(111) [5,15], one can assume that smoothness is a general phenomenon for Ag electrodeposition. Of course, less well defined substrates and high current densities can, in contrast, lead to very rough and even dendritic deposits that are encountered in Ag electrowinning.

4. Summary

STM and voltammetry show that Ag from $AgClO_4/HClO_4$ solutions deposits on Pt(100) in a very special upd phenomenon. After the upd of a single layer, with some second-layer islands that are pinned to substrate defects, coalescing islands of a well defined second layer build up about half a layer. The existence of islands suggests little perchlorate adsorption and attractive forces between Ag adatoms, reminiscent of the conditions encountered for vacuum deposition. The second upd takes place at potentials of only several millivolts positive of the bulk deposition. The Ag nucleation appears to occur at steps as well as on terraces. Comparable to a theoretical study and to the situation in Ag(100) homoepitaxy in vacuum, the growth is governed by rapid adatom diffusion. A third deposition process at a more negative potential almost completes the second layer before bulk growth sets in. In this way at least two layers of Ag can be grown without the use of surfactants.

Acknowledgements

I would like to thank G. Ertl and J. Wintterlin (FHI Berlin) for providing the opportunity for conducting the experiments and K. Bromann and S.E. Gilbert (EPFL) for their helpful comments.

References

[1] O.M. Magnussen, J. Hotlos, R.J. Nichols, D.M. Kolb, R.J. Behm, Phys. Rev. Lett. 64 (1990) 2929.
[2] O.M. Magnussen, J. Hotlos, G. Beitel, D.M. Kolb, R.J. Behm, J. Vac. Sci. B 9 (1991) 969.
[3] K. Sashikata, N. Furuya, K. Itaya, J. Electroanal. Chem. 316 (1991) 361.
[4] T. Hachiya, H. Honbo, K. Itaya, J. Electroanal. Chem. 315 (1991) 275.
[5] T. Hachiya, K. Itaya, Ultramicroscopy 42–44 (1992) 445.
[6] M.P. Green, K.J. Hanson, J. Vac. Sci. Technol. A 10 (1992) 3012.
[7] N. Ikemiya, S. Niyaoka, S. Hara, Surf. Sci. 311 (1994) L641.
[8] R.J. Nichols, D.M. Kolb, R.J. Behm, J. Electroanal. Chem. 313 (1991) 109.
[9] W. Haiss, J.K. Sass, D. Lackey, M. van Heel, in: S.H. Cohen et al. (Eds.), Atomic Force Microscopy/Scanning Tunneling Microscopy, Plenum Press, New York, 1994, p. 423.
[10] O.M. Magnussen, Ph.D. Thesis, Univ. Ulm, 1993.
[11] A.M. Bittner, J. Wintterlin, B. Beran, G. Ertl, Surf. Sci. 335 (1995) 291.
[12] A.M. Bittner, J. Wintterlin, G. Ertl, J. Electroanal. Chem. 388 (1995) 225.
[13] O.M. Magnussen, J. Hageböck, J. Hotlos, R.J. Behm, Faraday Discuss. 94 (1992) 329.
[14] C. Chen, S.M. Vesecky, A.A. Gewirth, J. Am. Chem. Soc. 114 (1992) 451.
[15] K. Ogaki, K. Itaya, Electrochim. Acta 40 (1995) 1249.
[16] N. Kimizuka, K. Itaya, Faraday Discuss. 94 (1992) 117.

[17] F. El Omar, R. Durand, R. Faure, J. Electroanal. Chem. 160 (1984) 385.
[18] J.L. Stickney, S.D. Rosasco, D. Song, M.P. Soriaga, A.T. Hubbard, Surf. Sci. 130 (1983) 326.
[19] F.A. Möller, O.M. Magnussen, R.J. Behm, Phys. Rev. B 51 (1995) 2484.
[20] A.M. Bittner, J. Wintterlin, G. Ertl, Surf. Sci. (1997) in press.
[21] M.S. Zei, N. Batina, D.M. Kolb, Surf. Sci. 306 (1994) L519.
[22] K. Wu, M.S. Zei, in prep. (1997).
[23] M. Dietterle, T. Will, D.M. Kolb, Surf. Sci. 327 (1995) L495.
[24] Y. Suzuki, H. Kikuchi, N. Koshizuka, Jpn. J. Appl. Phys. 27 (1988) L1175.
[25] C.-M. Zhang, M.C. Bartelt, J.-M. Wen, C.J. Jenks, J.W. Evans, P.A. Thiel, J. Crystal Growth (1997) in press.
[26] B.D. Yu, M. Scheffler, Phys. Rev. Lett. 77 (1996) 1095.